

Kai Bischof · Dieter Hanelt · Helmut Tüg · Ulf Karsten  
Patty E.M. Brouwer · Christian Wiencke

## Acclimation of brown algal photosynthesis to ultraviolet radiation in Arctic coastal waters (Spitsbergen, Norway)

Received: 13 March 1998 / Accepted: 16 May 1998

**Abstract** In field studies conducted at the Kongsfjord (Spitsbergen) changes of the irradiance in the atmosphere and the sublittoral zone were monitored from the beginning of June until the end of August 1997, to register the minimum and maximum fluxes of ultraviolet and photosynthetically active radiation and to characterise the underwater light climate. Measurements of photosynthesis in three abundant brown algal species (*Alaria esculenta*, *Laminaria saccharina*, *Saccorhiza dermatodea*) were conducted to test whether their photosynthetic performance reflects changing light climate in accordance with depth. Plants sampled at various depths were exposed to controlled fluence rates of photosynthetically active radiation (400–700 nm), UV-A (320–400 nm) and UV-B (280–320 nm). Changes in photosynthetic performance during the treatments were monitored by measuring variable chlorophyll fluorescence of photosystem II. In each species, the degree of inhibition of photosynthesis was related to the original collection depth, i.e. shallow-water isolates were more resistant than plants from deeper waters. The results show that macroalgae acclimate effectively to increasing irradiance levels for both photosynthetically active and ultraviolet radiation. However, the kinetics of acclimation are different within the different species. It is shown that one important strategy to cope with higher irradiance levels in shallow waters is the capability for a faster recovery from high light stress compared to isolates from deeper waters.

### Introduction

Macroalgae from high-Arctic coastal ecosystems inhabit a highly variable environment (Kirst and Wiencke 1995). Seasonal changes of abiotic factors include differences in temperature, mechanical disturbance (e.g. due to floating ice), salinity and nutrient levels. In particular, the light climate in polar coastal waters is subject to great seasonal changes. The different components of the spectrum are affected by several atmospheric (e.g. solar angle, clouds, aerosols, stratospheric ozone) and hydrographic [e.g. ice coverage, depth, dissolved organic material (DOM), sediment, detritus, phytoplankton] factors (Karentz 1989; Kirk 1994; Kirst and Wiencke 1995; Vosjan et al. 1996).

Generally, turbid waters are hardly transparent for ultraviolet radiation (UVR). As a result, only macroalgae growing in clear waters are likely to be affected by the harmful short wavelength range. Seasonal growth activity of Arctic macroalgal species coincides with high water transparencies in spring and, consequently, with higher UV-B (280–320 nm) and UV-A (320–400 nm) radiation in the water column (Holm-Hansen et al. 1993).

It is obvious that exposure of marine macrophytes to solar radiation is also dependent on the respective growth site and its microclimate. There are different possibilities as to how low-light-adapted plants can be protected against high fluence rates. One strategy is to grow below the canopy in the shade of for example, rocks or other plants. Another aspect is the restriction of growth to deeper waters at low penetration of UV. Only algae that own efficient protecting mechanisms and those that are capable of acclimating to high UV radiation have a chance of growing in shallow waters. With increasing depth, the fluence rates are exponentially diminished, and the original solar spectrum is strongly altered (Kirk 1994). Apart from highly specialised low-light-adapted plants (predominantly red algae), there are many Arctic macroalgal species growing over a wide depth range (Svendson 1959).

K. Bischof (✉) · D. Hanelt · H. Tüg · U. Karsten · C. Wiencke  
Alfred Wegener Institute for Polar and Marine Research,  
D-27515 Bremerhaven, Germany  
e-mail: kbischof@awi-bremerhaven.de,  
Fax: ++49/(0)471/4831-425

P.E.M. Brouwer  
Netherlands Institute for Ecology,  
4400 AC Yerseke,  
The Netherlands

In Antarctic macroalgae, genetic adaptation to high light stress is a major factor controlling depth distribution on the shore (Hanelt et al. 1997a; Bischof et al. in press). Some species have the genetic potential for acclimation to changing light conditions, which enables specimens to resist under high, as well as under low, light conditions and to photosynthesise efficiently in light climates with different spectral properties (Bischof et al. in press). Acclimation is achieved by alterations to pigment concentrations and ratios (Kirk 1994) and by adjustment of the light harvesting system, as well as the carboxylating process, to the respective radiation conditions (Lizotte and Sullivan 1991; Arrigo and Sullivan 1992).

Excessive absorbed energy may cause damage to the photosynthetic apparatus. The photodamage may differ in different wavelength ranges. High photosynthetically active radiation (PAR) increases the oxidative stress on proteins and pigments (e.g. D1-protein, chlorophylls) (Andersson et al. 1992). Also, enhanced UV may affect the function of the CO<sub>2</sub>-binding enzyme RubisCO (Strid et al. 1990; Nogues and Baker 1995) and formation and function of the D1-protein (Neale et al. 1993; Long et al. 1994), predominantly by the splitting of disulfide and peptide bonds. Also, UV can induce the formation of thymine dimers in nucleic acids (Karentz et al. 1991; Neale et al. 1993).

Dynamic photoinhibition can be regarded as one mechanism for protecting photosynthesis under the conditions of high PAR and UV radiation (Hanelt et al. 1994, 1997a; Hanelt 1996). It is defined as an actively regulated process (Krause and Weis 1991; Hanelt et al. 1993, 1994; Osmond 1994). During dynamic photoinhibition excessive energy is harmlessly dissipated as heat in the antenna complex causing reduced photosynthetic efficiency, which is fully reversible on a short time scale when the radiation stress decreases (Krause and Weis 1991). In contrast, chronic photoinhibition leads to inactivation of the D1-protein in the reaction centre of PS II, thus reducing the photosynthetic capacity for much longer time periods. Recovery after offset of excessive radiation is reflected by the de novo synthesis of the D1-protein.

In this study inhibition and recovery of photosynthesis was monitored in macroalgae from different water depths after transferring to treatments with controlled fluence rates of PAR, UV-A and UV-B radiation. The differences in photosynthetic activity measured are the result of acclimation to the respective light climates at the various water depths.

## Materials and methods

### Study sites

The investigations were performed at the Kongsfjord at the northwestern coast of Spitsbergen (Norway). Measurements of radiation and photosynthesis were carried out in the area of Ny Ålesund (78°55.5'N; 11°56.0'E Fig. 1.).

### Radiation measurements

PAR at the surface was measured using an LI-COR cosinus flat-head sensor (Quantum, Lincoln, USA) connected to a datalogger (LI-COR, LI-1000). Underwater measurements of PAR were monitored by means of two LI-COR cosinus flat-head sensors. For determination of diffuse vertical attenuation coefficients of downward irradiance ( $K_d$ ), the two sensors were placed at different depths and the ratios of fluence rates were detected.  $K_d$  was calculated using the following formula (Kirk 1994):

$$K_d = 1/(z_1 - z_2) * \ln E_{d(z_1)}/E_{d(z_2)}$$

with  $E_{d(z_1)}$  and  $E_{d(z_2)}$  as the respective irradiance at depth  $z_1$  and  $z_2$ .

UV-B radiation (280–320 nm) in air was measured using a 32-channel single photon counting radiometer developed at the Alfred Wegener Institute and installed on the roof of the NDSC building (Network for the Detection of Stratospheric Changes, Koldewey Station, Alfred Wegener Institute). In the experimental set-ups, artificial UV radiation emitted by special fluorescence tubes (see below) was measured with an RM-21 bandpass radiometer equipped with broadband  $2\pi$  UV-A (320–400 nm) and UV-B (280–320 nm) sensors (Dr. Gröbel, Germany). The instrument was intercalibrated with a spectroradiometer (Spectro 320 D, Instrument Systems, Germany) checked against a calibration lamp. UV-B radiation inside the water column was recorded via the same type of multi-channel radiometer as mentioned above but in a pressure housing. This instrument was constructed for continuous and single measurements of fluence rates in the UV-B range. The instrument floated in the water column and was fixed to a pulley anchored at the ground of the fjord, so that depth profiles of UV-B penetration were recorded by drawing the instrument into the respective depth. The instrument was computer controlled allowing on-line recordings of the data. Also, for UV-B radiation,  $K_d$  was calculated as described above.

### Plant material

All plants used in the experiments were collected by scuba diving at Hansneset (Blomstrand Island, Kongsfjord). Each species was collected at a range of different depths (Table 1). Under water, the

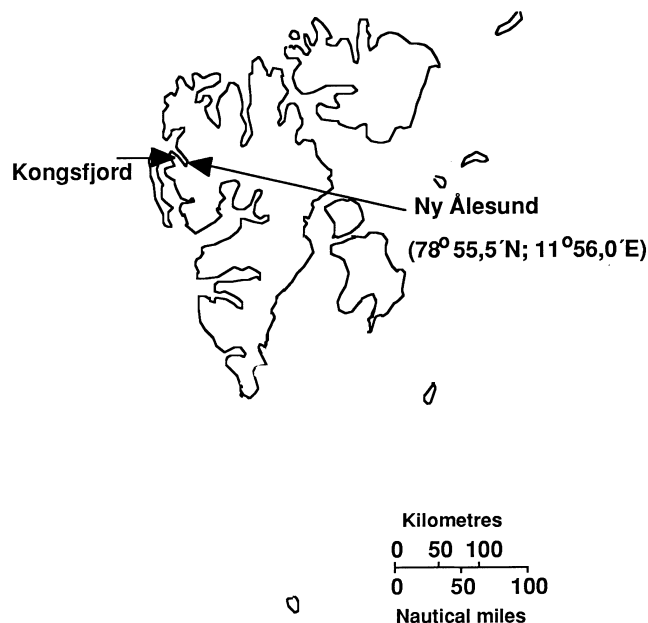


**Fig. 1** Location of the study site on Spitsbergen archipelago (Svalbard)

**Table 1** Investigated species and sampling depth

Species	Sampling depth (m)
<i>Alaria esculenta</i> (L.) Grev.	2, 4.5, 7, 10
<i>Laminaria saccharina</i> (L.) Lamour.	3, 6, 11, 14/3, 5, 7, 9, 11, 13
<i>Saccorhiza dermatodea</i> (Pyl.) J. Ag.	3, 6, 9, 11

**Table 2** Exposure conditions

Condition of exposure
1. 12 h of pre-cultivation in dim white light ( $20 \mu\text{mol} \cdot \text{m}^{-2} \cdot \text{s}^{-1}$ )
2. 4 h of exposure to $60 \mu\text{mol} \cdot \text{m}^{-2} \cdot \text{s}^{-1}$ PAR (filter GG 400) or to $60 \mu\text{mol} \cdot \text{m}^{-2} \cdot \text{s}^{-1}$ PAR + $7 \text{ W} \cdot \text{m}^{-2}$ UV-A (filter WG 320) or to $60 \mu\text{mol} \cdot \text{m}^{-2} \cdot \text{s}^{-1}$ PAR + $7 \text{ W} \cdot \text{m}^{-2}$ UV-A + $0.7 \text{ W} \cdot \text{m}^{-2}$ UV-B (filter WG 280)
3. 24 h of recovery in dim white light ( $20 \mu\text{mol} \cdot \text{m}^{-2} \cdot \text{s}^{-1}$ )

plants were put into a black bag to avoid exposure to higher irradiances when being transported to the water surface right after collection. The individual plants were of equal size and morphology. After sampling, the plants were kept (in basins with running seawater of the same salinity and temperature as at the collecting site) in the laboratory for 12 h in dim white light ( $20 \mu\text{mol} \cdot \text{m}^{-2} \cdot \text{s}^{-1}$ ), generated by Philips daylight fluorescence tubes. For irradiation experiments, pieces of tissue were cut from the middle of each thallus and transferred to the experimental set-ups.

#### Experimental set-ups and exposure conditions

To study acclimation of photosynthesis to the respective light climate in plants collected from different water depths, all samples were exposed to the same radiation conditions. Photosynthetically active radiation was provided by Philips daylight fluorescence tubes with fluence rates of  $60 \mu\text{mol} \cdot \text{m}^{-2} \cdot \text{s}^{-1}$ . UV radiation similar to the spectrum of the sun between 300 and 345 nm was provided by 2 Q-Panel UVA-340 fluorescence tubes (Cleveland, USA) at irradiances of  $7 \text{ W} \cdot \text{m}^{-2}$  UV-A (320–400 nm) and  $0.7 \text{ W} \cdot \text{m}^{-2}$  UV-B (280–320 nm). Each sample was exposed to three different light regimes representing different spectral ranges (PAR, PAR + UV-A, PAR + UV-A + UV-B). This was achieved by using Schott cut-off filters (GG 400, WG 320, WG 280). The plants were exposed for 4 h to each radiation condition and were subsequently transferred to dim white light for 24 h to induce recovery. The exposure conditions are summarised in Table 2.

#### Measurements of photosynthesis

Photosynthetic activity was determined by measuring variable chlorophyll-fluorescence of PS II with a PAM-2000 device (Walz, Effeltrich, Germany). Optimum quantum yield was calculated as the ratio of variable to maximum fluorescence ( $F_v/F_m$ ) of the dark-acclimated plant. Small pieces cut from the thalli were fixed to the end of the fiberoptics, and placed in a cooled cuvette filled with seawater. After application of a 5-s far-red pulse ( $30 \mu\text{mol} \cdot \text{m}^{-2} \cdot \text{s}^{-1}$  at 735 nm), the samples were kept in darkness for 5 min. Afterwards, minimal fluorescence ( $F_o$ ) was measured with a pulsed measuring beam (approximately  $0.3 \mu\text{mol} \cdot \text{m}^{-2} \cdot \text{s}^{-1}$ , 650 nm). Then short pulses of saturating white light (0.4–0.8 s, 1500 up to

$10,000 \mu\text{mol} \cdot \text{m}^{-2} \cdot \text{s}^{-1}$ ) were provided to determine  $F_m$ . Optimum quantum yield was measured after 0, 0.5, 1, 2 and 4 h of exposure and after 2, 4 and 24 h of recovery.

To determine changes in the photosynthetic capacity, photosynthesis versus irradiance curves (PI-curve) were calculated. Samples were irradiated with increasing irradiance of actinic red light ( $10\text{--}700 \mu\text{mol} \cdot \text{m}^{-2} \cdot \text{s}^{-1}$ , 650 nm). After 30 s a saturating pulse was applied to measure effective quantum yield of photosynthesis ( $\Delta F/F_m'$  c.f. Genty et al. 1989) and then actinic irradiation was increased. By multiplying quantum yield with photon fluence rate (PFR) relative electron transport rates were calculated as described by Schreiber et al. (1994):  $\text{rel. ETR} = \Delta F/F_m' \cdot \text{PFR}$ . These were plotted against irradiance of actinic light, and maximal relative electron transport rate (ETR<sub>max</sub>, under saturating light) was determined by curve-fitting. PI-curves were monitored after 0 and 4 h of exposure and after 24 h of recovery.

#### Data treatment

Mean values and standard deviations were calculated from four replicates per treatment. The means of unstressed controls of the respective sampling depth were normalised to 100%, allowing a better comparison among different samples. Statistical significance of differences in photoinhibitory response and recovery in plants from different depths was tested by one-way analysis of variance (ANOVA). Homogeneity of variance was tested by a F-test. Calculations were done using the program Stat View 4.5.

## Results

### Radiation measurements

Due to the high latitude, the angle of the sun is low even in mid-summer at noon. Maximum values of PAR were  $1300 \mu\text{mol} \cdot \text{m}^{-2} \cdot \text{s}^{-1}$  on 15 June 1997. Maximum irradiation of UV-A (320–400 nm) in air was  $19 \text{ W} \cdot \text{m}^{-2}$  and  $1.09 \text{ W} \cdot \text{m}^{-2}$  UV-B (280–320 nm) on the same day. Radiation inside the water column was subject to many changes also on a short time scale. Daily measurements of air temperature (10 m above sea level; data not shown) revealed that from 8 June 1997 surface temperature rose permanently above  $0^\circ\text{C}$  resulting in the thawing of snow and input of turbid melt-water from streams and glaciers close to the bay. As is usual for most Arctic coastal waters during this time, transmittance in the Kongsfjord was not very high and changed dramatically with the season. Maximum light penetration was observed just before the start of the snow melting with a maximum transmittance in the PAR range, with  $K_d$  value,  $0.19 \text{ m}^{-1}$ , measured on 14 June 1997. Minimum transmittance for PAR was measured on 16 July 1997 ( $K_d$ :  $0.74 \text{ m}^{-1}$ ). Within this range of maximum and minimum values, light transmittance varied greatly with the measuring site and time (e.g. by the inflow of melt-water streams), especially for UV radiation inside the water column, as short wavelengths are much more scattered and absorbed by turbid water and DOM. One example of UV-B penetration into the fjord is shown in Fig. 2. These measurements were made when atmospheric UV-B radiation was maximal in air ( $1.09 \text{ W} \cdot \text{m}^{-2}$ ). The spectrum recorded above the water

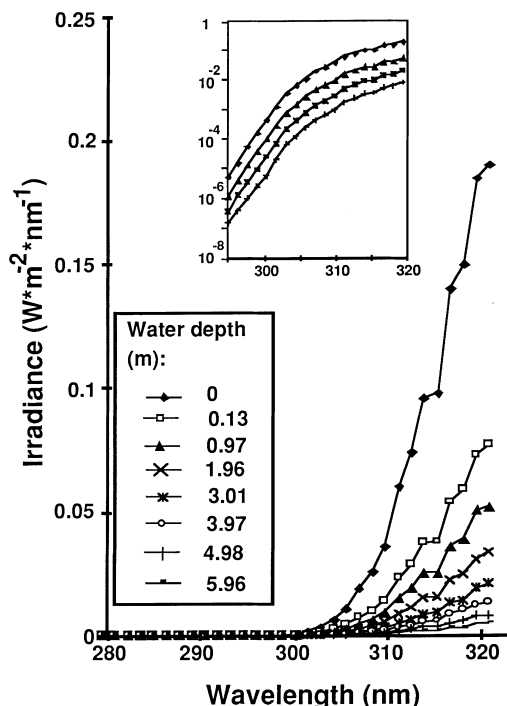


**Fig. 2** UV-B radiation (280–320 nm) in the water column, measured on 15 June 1997; 12 noon. *Inset* shows the radiation at 0-, 0.97-, 3.01- and 4.98-m depth with a logarithmic scale

surface (0 m) shows that even under the highest irradiances of UV-B only very low radiation below 300 nm was detected. The measurement recorded at 0.13-m depth shows the rapid attenuation of UV-B radiation. Within the first 0.13-m approximately 70% of the surface UV-B radiation is lost. Maximum transmittance of UV-B radiation was measured on 14 June 1997 ( $K_d$ :  $0.51 \text{ m}^{-1}$ ); minimum transmittance was observed on 16 July 1997 ( $K_d$ :  $1.34 \text{ m}^{-1}$ ). The radiation data are summarised in Table 3.

## Photosynthesis

Photosynthetic performance of the individual plants was affected differently by UV radiation depending on the species and water depth. As one example, the PI-curves shown in Fig. 3 revealed the differences in photosyn-

thetic performance after exposing individuals of *Laminaria saccharina* from different water depths for 4 h to the full radiation spectrum in the experiment. Relative electron transport rates, measured after 4 h of exposure to PAR + UV-A + UV-B, were referred to ETRmax values of controls from the respective sampling depth. It is obvious that photosynthetic rates in plants from deeper waters were significantly reduced in accordance with the original growth depth, and that photosynthesis in the sample from 3-m depth was unaffected.

The changes in optimum quantum yield during the different treatments are summarised in Fig. 4a. The plants collected from greater depth were more sensitive to the additional UV irradiation in all light treatments than isolates from shallow waters. Strong inhibitory effects directly after exposure to UV-A and UV-B radiation were visible, but were more pronounced in the full spectrum. Optimum quantum yield in plants exposed to the full spectrum was inhibited in accordance with sampling depth. These differences were not found in the samples exposed to PAR + UV-A. After additional post-cultivation to dim white light for 24 h the degree of recovery of optimum quantum yield was significantly related to the original growth depth of samples. This correlation between recovering capacity and depth of

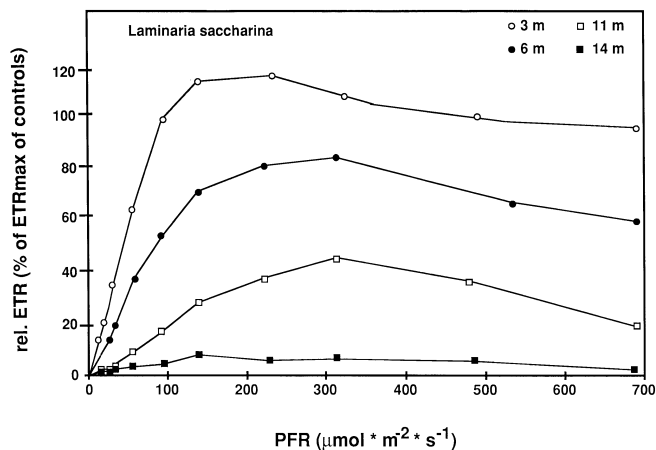


**Fig. 3** Photosynthetic performance of *Laminaria saccharina* from four different depths after 4 h of exposure to PAR + UVA + UVB. *PFR* is the respective photon fluence rate of actinic white light and *ETR* is the electron transport rate. Relative *ETR* is expressed as % of *ETR*max values in controls, sampled from the respective growth site

**Table 3** Radiation measurements

Measurement of radiation			
Atmosphere			
Max. PAR	15 June 1997	12 noon	$1300 \mu\text{mol} \cdot \text{m}^{-2} \cdot \text{s}^{-1}$
Max. UV-A	15 June 1997	12 noon	$19 \text{ W} \cdot \text{m}^{-2}$
Max. UV-B	15 June 1997	12 noon	$1.09 \text{ W} \cdot \text{m}^{-2}$
Water column			
PAR: max. transmittance	14 June 1997	$K_{d\text{PAR}} = 0.19 \text{ m}^{-1}$	1% depth: 24.2 m
PAR: min. transmittance	16 July 1997	$K_{d\text{PAR}} = 0.74 \text{ m}^{-1}$	1% depth: 6.2 m
UV-B: max. transmittance	14 June 1997	$K_{d\text{UV-B}} = 0.51 \text{ m}^{-1}$	1% depth: 9.0 m
UV-B: min. transmittance	16 July 1997	$K_{d\text{UV-B}} = 1.34 \text{ m}^{-1}$	1% depth: 3.4 m

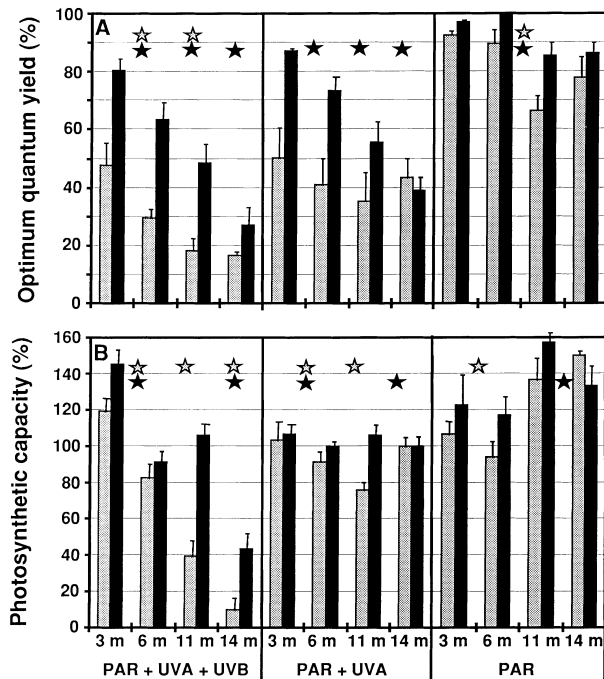


**Fig. 4A,B** Changes in optimum quantum yield (A) and photosynthetic capacity (B) in *L. saccharina*, expressed as % of control values. The different light regimes were achieved by covering the samples with the respective cut-off filters (GG 400, WG 320; WG 280) as stated in Materials and methods. Grey bars: after 4 h exposure; black bars: after 24 h recovery. Significant differences among samples from different depths are marked with stars ( $P < 0.0001$ )

sampling is shown in samples exposed to PAR + UV-A + UV-B and also in plants exposed under UV-B exclusion.

A clear inhibitory effect on photosynthetic capacity in *L. saccharina* was only found with exposure to PAR + UV-A + UV-B radiation. An exception was the sample collected from 3-m depth, where ETRmax was stimulated by the radiation treatment. ETRmax values of the other samples were depressed in relation to their sampling site (Fig. 4b). In the sample from 14-m depth, recovery of photosynthetic capacity was not completed after 24 h in dim white light.

In order to analyse the contribution of each wavelength range to the inhibitory effect, the changes in ETRmax values measured under different treatments are plotted in a series of pairwise comparisons (Fig. 5). Large positive values illustrate a great additional contribution of UV radiation to changes in photosynthetic capacity. UV-A and UV-B radiation synergistically caused significant inhibition of photosynthetic capacity in accordance with the respective growth depth of samples (Fig. 5a). Inhibition due to UV-A radiation was only present in the samples from 11- and 14-m depth, but the extent of inhibition was similar in samples from both depths (Fig. 5b). In the samples from 6- and 11-m depth, additional UV-B effects were small, especially after 24 h of recovery (Fig. 5c). However, the samples

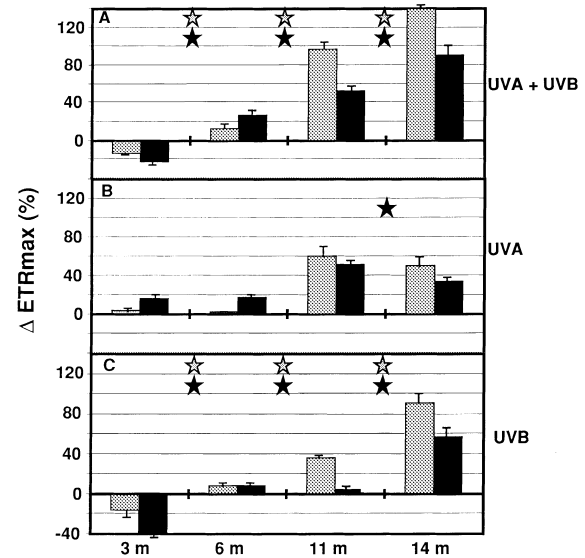


**Fig. 5A–C** Contribution of different wavelength ranges to the overall inhibition of photosynthetic capacity in *L. saccharina* expressed as the difference in ETRmax values (% of control values) measured under PAR and PAR + UVA + UVB treatment (A), PAR and PAR + UVA treatment (B), and PAR + UVA and PAR + UVA + UVB treatment (C). Further details as in legend to Fig. 4. Grey bars: after 4 h exposure; black bars: after 24 h recovery. Significant differences among samples from different depths are marked with stars ( $P < 0.0001$ )

from 14-m depth were strongly affected. UV-B radiation caused an increase of the photosynthetic capacity in the 3-m samples. Similar results were observed in measurements of the optimum quantum yield.

In an additional experiment individuals of *L. saccharina* were collected in 2-m steps from 3- to 13-m depth and exposed for 4 h to PAR + UV-A + UV-B (Fig. 6). During the inhibitory phase, no significant differences between the samples were observed. However, there was a trend to lower optimum quantum yields after exposure to UV and PAR with increasing depths. This trend is more obvious in the recovery experiments: the degree of recovery in plants from 3, 5, 7 and 9 m is significantly correlated with depth.

In *Saccorhiza dermatodea*, the differential sensitivity of individuals collected from different depths is predominantly visible in the optimum quantum yield (Fig. 7a). Exposure to PAR alone did not result in decreasing  $F_v/F_m$  values in any of the samples. In the samples exposed under the WG 320 filter, UV-A prevented recovery of the 11-m samples. The plants collected at 3, 6 and 9 m were inhibited but they recovered. Again, samples receiving the full spectrum are even more strongly inhibited directly after exposure but recovery was possible in the samples from 3, 6 and 9 m. However, it should be noted that the individuals of *S. dermatodea* growing in shallow waters were only small (half of the size of the algae collected at greater depth, probably due to abrasion by floating ice) and, hence, may differ in their response to the treatments from the larger indi-

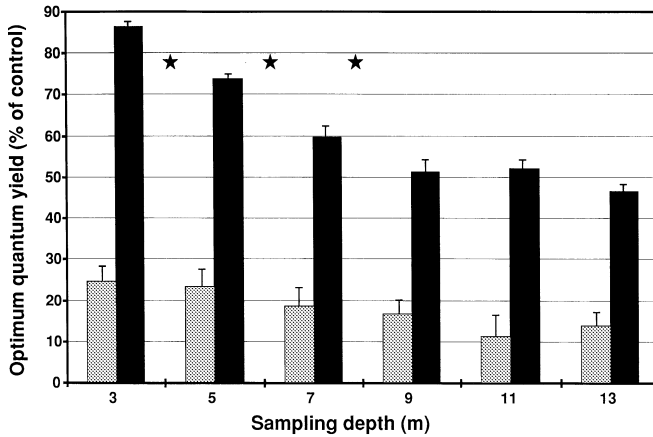


**Fig. 6** Changes in optimum quantum yield in *L. saccharina* collected in 2-m steps, expressed as % of control values. Grey bars: after 4 h exposure to PAR + UVA + UVB; black bars: after 24 h recovery. Significant differences among samples from different depths are marked with stars ( $P < 0.0001$ )

viduals from greater depth. Inhibition of optimum quantum yield in samples from this depth was greater than in plants from 6- and 9-m depth. However, recovery occurred to a similar extent in the sample from shallow water.

Optimum quantum yield was also affected in *Alaria esculenta* (Fig. 7b). Again, in this species a difference in response with respect to growth depth was obvious in the phase of recovery and not so clear in the inhibitory phase. This is especially shown for samples exposed to the full spectrum: the correlation between inhibition of optimum quantum yield and sampling depth is weak.

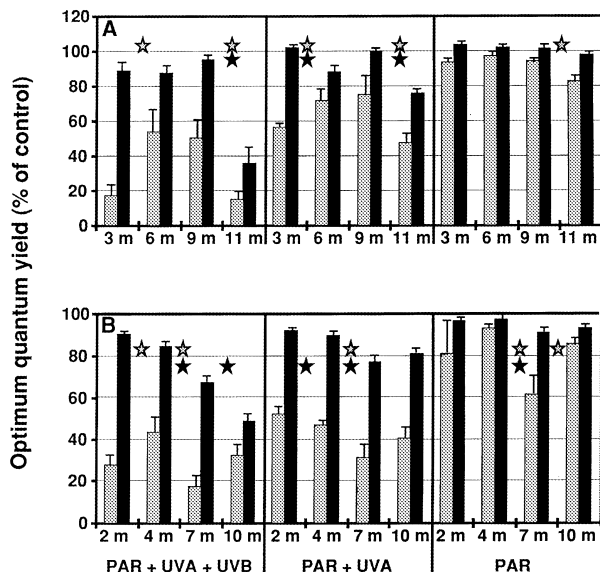


**Fig. 7A,B** Changes in optimum quantum yield in *Saccorhiza dermatodea* (A) and *Alaria esculenta* (B), expressed as % of control values. Further details as in legend to Fig. 4. Grey bars: after 4 h exposure; black bars: after 24 h recovery. Significant differences among samples from different depths are marked with stars ( $P < 0.0001$ )

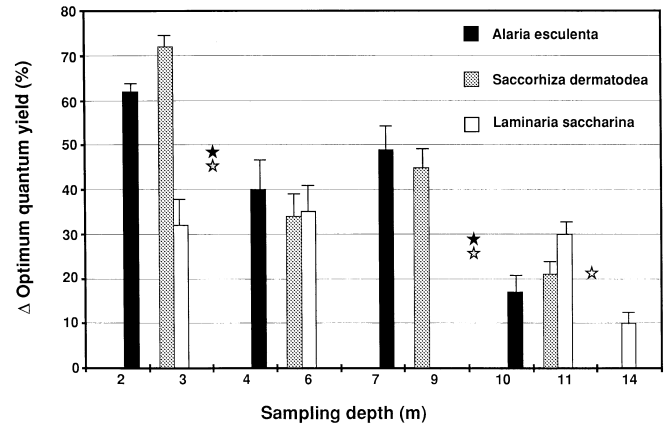


**Fig. 8** Recovery rate of optimum quantum yield, expressed as the difference between  $F_v/F_m$  values (% of control values) measured after 24 h recovery and 4 h exposure to PAR + UVA + UVB. Significant differences among samples from different depths are marked with stars ( $P < 0.0001$ )

For unknown reasons the samples from 2-m depth were inhibited more strongly than samples from 4 m, samples from 7-m depth were inhibited most strongly and plants collected at 10 m were inhibited to a similar extent as plants from 4 m. However, the degree of recovery was significantly less with increasing depth.

To summarise the results obtained with the chosen brown algal species, the rate of the recovery process expressed as the differences between optimum quantum yield measured after 24 h recovery and 4 h exposure to the full spectrum is plotted in Fig. 8. For all species it is shown that generally specimens from shallow water recover to a greater extent than those from deeper waters.

## Discussion

There is only scant information concerning light transmittance in coastal waters of the high Arctic. In a previous study the penetration of UV-B radiation into the water may have been underestimated (Hanelt et al. 1997c). This was partly due to the low accuracy of the available devices for underwater radiation measurements and the time of the year when this study was conducted. Although a large fraction of the impinging UV-B radiation is attenuated in the first centimetres of the water column or even reflected at the water surface (see Fig. 2), the present results show that in clear waters in Arctic spring UV-B radiation penetrates much deeper than previously estimated. The maximum penetration depth for UV-B radiation in the sublittoral zone of the Kongsfjord was at 10 m. However, in the off-shore waters of the North Atlantic 10% of the surface UV-B radiation was detected down to 10 m, which is in the same order as in Antarctic waters (Wängberg et al. 1996). Due to the changes in atmospheric (solar declination, cloud cover) and hydrographic factors, the

transmittance for any spectral range is highly variable in time and with the measuring site. Later in the year, air temperature at the northwestern coast of Spitsbergen can rise to approximately 15°C, resulting in much thawing of snow and calving of glaciers thus causing a high input of sediment into the fjord waters. Under these conditions optical transparency is very low.

The experimental set-up of this study was designed to test the reaction of macroalgae to enhanced UV-B radiation. The UV-B irradiance the samples were exposed to was similar to those values measured in clear waters at approximately 1-m depth on a sunny day. There is evidence that photosynthesis of macroalgae growing in shallow waters is generally less sensitive to high radiation (PAR and UV) than in deep-water algae (Henley et al. 1991; Larkum and Wood 1993; Franklin et al. 1996; Hanelt et al. 1997a). This can be due to genetic adaptation within different species or ecotypes (Hanelt et al. 1997a; Bischof et al. in press) and to acclimation to different light regimes (Hanelt 1998). As the radiation measurements inside the Kongsfjord show, plants collected at depths greater than 10-m are not exposed to harmful UV-B radiation.

Plants from these depths can only grow in shallow water after acclimation to higher irradiance levels. It is remarkable that the recovery rate after exposure to UV-B radiation differs greatly among samples of *Laminaria saccharina* collected at 11-m and 14-m (Fig. 4), as the light climate is only slightly different between these depths (Fig. 2). However, the high sensitivity to artificial UV radiation in plants from deeper waters and the higher tolerance of samples collected in shallow waters show that a potential for regulation of photosynthetic activity and acclimation to changing irradiances exists. Up to now there have been no reliable data available concerning the mechanisms for regulation or the period of time required for acclimation in marine macroalgae. For higher plants, a fast regulation of chloroplast metabolism due to redox modifications of protein-thiols is well described (Scheibe 1990). Future studies will have to elucidate which radiation conditions exceed the regulation and acclimation capacity and to work out the regulating mechanisms.

Differences in sensitivity were recorded for both optimum quantum yield and photosynthetic capacity, indicating that several mechanisms of inhibition may be involved. Decrease in photosynthetic efficiency is thought to be predominantly caused by reduced light-harvesting efficiencies in the antennae complexes resulting in heat dissipation of excessively absorbed energy (Krause and Weis 1991). Changes in photosynthetic capacity are attributed to an inactivation of PS II reaction centres (Mattoo et al. 1984), but also to lower activities of enzymes of the Calvin cycle, predominantly RubisCO (Strid et al. 1990; Nogues and Baker 1995). The response of the inhibitory phase during exposure to high radiation should be carefully distinguished from the recovery phase. Especially under natural exposure conditions, UV radiation causes a delay in recovery rather

than an additional inhibition of photosynthesis of Arctic macroalgae (Hanelt et al. 1997c). Different protective mechanisms are described for protection against UV radiation but most of them are only effective in the inhibitory phase during exposure. Differences in morphology such as, for instance, increasing thallus thickness may be regarded as one protective mechanism against both high PAR and UVR in macroalgae (Dring et al. 1996; Hanelt et al. 1997b) as well as in seagrasses (Dawson and Dennison 1996). This might explain why photosynthetic efficiency in *Saccorhiza dermatodea* from 3-m depth was inhibited to a similar degree as the sample from 11 m after 4 h of exposure under the WG 280 filter (Fig. 6a). This may be related to the morphology of the thalli: the samples from shallow water were much smaller and thinner, probably allowing the radiation to penetrate much better to the chloroplasts, resulting in greater inhibition of photosynthesis. However, fast restoration of  $F_v/F_m$  values in the 3-m samples show the high capability of photosynthesis to recover from harmful radiation conditions. This is clearly absent in the sample from 11-m depth.

Chloroplast movement can also reduce absorption of harmful excessive energy in brown algae (Nultsch and Pfau 1979; Hanelt and Nultsch 1990), but does not protect against UV radiation (Hanelt and Nultsch 1989). Differences in pigmentation (e.g. chlorophyll/carotenoid ratios), as well as the presence of special UV screening substances [e.g. Mycosporine-like amino acids (MAAs) in red algae], can account for differences in photosynthetic performance during the inhibitory phase. Karsten et al. (1998) have already shown the inducibility of MAA synthesis in the red algae *Chondrus crispus* in response to changing radiation. Phenolic compounds (e.g. phlorotannins) are reported to serve as UV screening substances in brown algae such as *Ascophyllum nodosum* (Pavia et al. 1997). In the brown alga *Ecklonia radiata* it was shown that the concentrations of UV absorbing substances change seasonally and are significantly correlated with UV flux at sea level and PAR and UV flux at 5-m depth (Wood 1987).

As our results show, one important strategy to cope with higher irradiances at lower depth is to optimise regulatory mechanisms to reduce the required time for recovery from high light stress. For *Laminaria saccharina* especially it is shown that the capacity to recover from exposure to high radiation is clearly related to the light climate at the growth site (Figs. 4, 6). Different kinetics of recovery from photoinhibition in plants from different depths were recently described by Hanelt (1998). The strategies listed above to reduce the impact of high radiation can only account for the inhibitory phase, and not for any differences in the rate of recovery. Although the mechanisms are still unknown it seems more likely that this acclimation could be achieved by the different expression or activity of repair processes (e.g. photolyase, D1-turnover rates). For this, future studies should focus on the enzymatic processes involved.

**Acknowledgements** The authors are most grateful to Heike Lippert and Barbara Vögele for providing samples by scuba diving. Thanks also go to Michael Roßbach for his help conducting the experiments. We are indebted to the European Commission (Project ENV4-CT96-0188, DG12) for financial support. The practical works were performed in 1997 at the Ny Ålesund International Research and Monitoring Facility. This is contribution no. 1428 of the Alfred Wegener Institute for Polar and Marine Research.

## References

- Andersson B, Salter AH, Virgin I, Vass I, Styring S (1992) Photodamage of photosystem II – primary and secondary events. *J Photochem Photobiol B Biol* 15:15–31
- Arrigo KR, Sullivan CW (1992) The influence of salinity and temperature covariation on the photophysiological characteristics of Antarctic sea ice microalgae. *J Phycol* 28:746–756
- Bischof K, Hanelt D, Wiencke C (in press) UV-radiation can affect depth-zonation of Antarctic macroalgae. *Mar Biol*
- Dawson SP, Dennison WC (1996) Effects of ultraviolet and photosynthetically active radiation on five seagrass species. *Mar Biol* 125:629–638
- Dring MJ, Makarov V, Schoschina E, Lorenz M, Lüning K (1996) Influence of ultraviolet radiation on chlorophyll fluorescence and growth in different life history stages of three species of *Laminaria* (Phaeophyta). *Mar Biol* 126:183–191
- Franklin LA, Seaton GGR, Lovelock CE, Larkum AWD (1996) Photoinhibition of photosynthesis on a tropical reef. *Plant Cell Environ* 19:825–836
- Genty B, Briantais JM, Baker NR (1989) The relationship between the quantum yield of photosynthetic electron transport and quenching of chlorophyll fluorescence. *Biochim Biophys Acta* 990:87–92
- Hanelt D (1996) Photoinhibition of photosynthesis in marine macroalgae. *Sci March* 60:243–248
- Hanelt D (1998) The capability for dynamic photoinhibition in Arctic macroalgae is related to their depth distribution. *Mar Biol* 131:361–369
- Hanelt D, Nultsch W (1989) Action spectrum of phaeoplast displacements from the dark to the low intensity arrangement in the brown alga *Dictyota dichotoma*. *J Photochem Photobiol B Biol* 4:111–121
- Hanelt D, Nultsch W (1990) Daily changes of the phaeoplast arrangement in the brown alga *Dictyota dichotoma* as studied in field experiments. *Mar Ecol Prog Ser* 61:273–279
- Hanelt D, Huppertz K, Nultsch W (1993) Daily course of photosynthesis and photoinhibition in marine macroalgae investigated in the laboratory and field. *Mar Ecol Prog Ser* 97:31–37
- Hanelt D, Jaramillo MJ, Nultsch W, Senger S, Westermeier R (1994) Photoinhibition as a regulative mechanism of photosynthesis in marine algae of Antarctica. *Ser Cient INACH* 44:76–77
- Hanelt D, Melchersmann B, Wiencke C, Nultsch W (1997a) Effects of high light stress on photosynthesis of polar macroalgae in relation to depth distribution. *Mar Ecol Prog Ser* 149:255–266
- Hanelt D, Wiencke C, Karsten U (1997b) Photoinhibition and recovery after high light stress in different developmental and life-history stages of *Laminaria saccharina* (Phaeophyta). *J Phycol* 33:387–395
- Hanelt D, Wiencke C, Nultsch W (1997c) Influence of UV radiation on photosynthesis of Arctic macroalgae in the field. *J Photochem Photobiol B Biol* 38:40–47
- Henley WJ, Levavasseur G, Franklin LA, Lindley ST, Ramus J, Osmond CB (1991) Diurnal responses of photosynthesis and fluorescence in *Ulva rotundata* acclimated to sun and shade in outdoor culture. *Mar Ecol Prog Ser* 75:19–28
- Holm-Hansen O, Lubin D, Helbling EW (1993) Ultraviolet radiation and its effects on organisms in aquatic environments. In: Young AR, Björn LO, Moan J, Nultsch W (eds) *Environmental UV photobiology*. Plenum, New York, pp 379–425
- Karentz D (1989) Report on studies related to the ecological implications of ozone depletion on the Antarctic environment. *Antarct J US* 24:175–176
- Karentz D, Cleaver JE, Mitchell DL (1991) Cell survival characteristics and molecular responses of Antarctic phytoplankton to ultraviolet-B radiation. *J Phycol* 27:326–341
- Karsten U, Franklin LA, Lüning K, Wiencke C (1998) Natural ultraviolet and photosynthetic active radiation induce formation of mycosporine-like amino acids in the marine macroalga *Chondrus crispus* (Rhodophyta). *Planta* 205:257–262
- Kirk JTO (1994) *Light and photosynthesis in aquatic ecosystems*, 2nd edn. Cambridge University Press, Cambridge
- Kirst GO, Wiencke C (1995) Ecophysiology of polar algae. *J Phycol* 31:181–199
- Krause GH, Weis E (1991) Chlorophyll fluorescence and photosynthesis: the basics. *Annu Rev Plant Physiol Plant Mol Biol* 42:313–349
- Larkum AWD, Wood WF (1993) The effect of UV-B radiation on photosynthesis and respiration of phytoplankton, benthic macroalgae and seagrasses. *Photosynth Res* 36:17–23
- Lizotte MP, Sullivan CW (1991) Rates of photoadaptation in sea ice diatoms from McMurdo Sound, Antarctica. *J Phycol* 27:367–373
- Long SP, Humphries S, Falkowski PG (1994) Photoinhibition of photosynthesis in nature. *Annu Rev Plant Physiol Plant Mol Biol* 45:633–662
- Mattoo AK, Hoffman-Falk H, Marder JB, Edelman M (1984) Regulation of protein metabolism: coupling of photosynthetic electron transport *in vivo* degradation of the rapidly metabolised 32-kilodalton protein of the chloroplast membranes. *Proc Natl Acad Sci USA* 81:1380–1384
- Neale PJ, Cullen JJ, Lesser MP, Melis A (1993) Physiological bases for detecting and predicting photoinhibition of aquatic photosynthesis by PAR and UV radiation. In: Yamamoto, Smith (eds) *Photosynthetic responses to the environment*. American Society of Plant Physiologists, Rockville, pp 61–77
- Nogues S, Baker NR (1995) Evaluation of the role of damage to photosystem II in the inhibition of CO<sub>2</sub> assimilation in pea leaves on exposure to UV-B radiation. *Plant Cell Environ* 18:781–787
- Nultsch W, Pfau JPM (1979) Occurrence and biological role of light-induced chromatophore displacement in seaweeds. *Mar Biol* 51:77–82
- Osmond CB (1994) What is photoinhibition? Some insights from comparisons of shade and sun plants. In: Baker NR, Bowyer NR (eds) *Photoinhibition of photosynthesis, from the molecular mechanisms to the field*. BIOS Scientific, Oxford, pp 1–24
- Pavia H, Cervin G, Lindgren A, Åberg P (1997) Effects of UV-B radiation and simulated herbivory on phlorotannins in the brown alga *Ascophyllum nodosum*. *Mar Ecol Prog Ser* 157:139–146
- Scheibe R (1990) Light/dark modulation: regulation of chloroplast metabolism in a new light. *Bot Acta* 103:327–334
- Schreiber U, Bilger W, Neubauer C (1994) Chlorophyll fluorescence as a noninvasive indicator for rapid assessment of *in vivo* photosynthesis. *Ecol Stud* 100:49–70
- Strid Å, Chow WS, Anderson JM (1990) Effects of supplementary ultraviolet-B radiation on photosynthesis in *Pisum sativum*. *Biochim Biophys Acta* 1020:260–268
- Svendson P (1959) The algal vegetation of Spitsbergen. *Norsk Polar Institutt Skrifter* no. 116, Oslo
- Vosjan JH, Van Balen ALH, Zdanowski MK (1996) Microbial biomass and light attenuation (PAR, UV-A, UV-B) in the Weddell Sea and the effect of UV-B on the ATP content of microbes. *Circumpolar J* 1-2:28–32
- Wängberg SA, Selmer JS, Ekelund NGA, Gustavson K (1996) UV-B effects on Nordic marine ecosystem. Tema Nord 1996. Nordic Council of Ministers, Copenhagen
- Wood WF (1987) Effect of solar ultra-violet radiation on the kelp *Ecklonia radiata*. *Mar Biol* 96: 143–150